

# КОНСТРУИРОВАНИЕ МАКРОМОЛЕКУЛ МЕТОДОМ ATRP



**Кузнецов Александр Алексеевич**

ИСПМ им. Н.С.Ениколопова РАН

Лекция подготовлена по обзору



Perspective

[pubs.acs.org/JACS](https://pubs.acs.org/JACS)

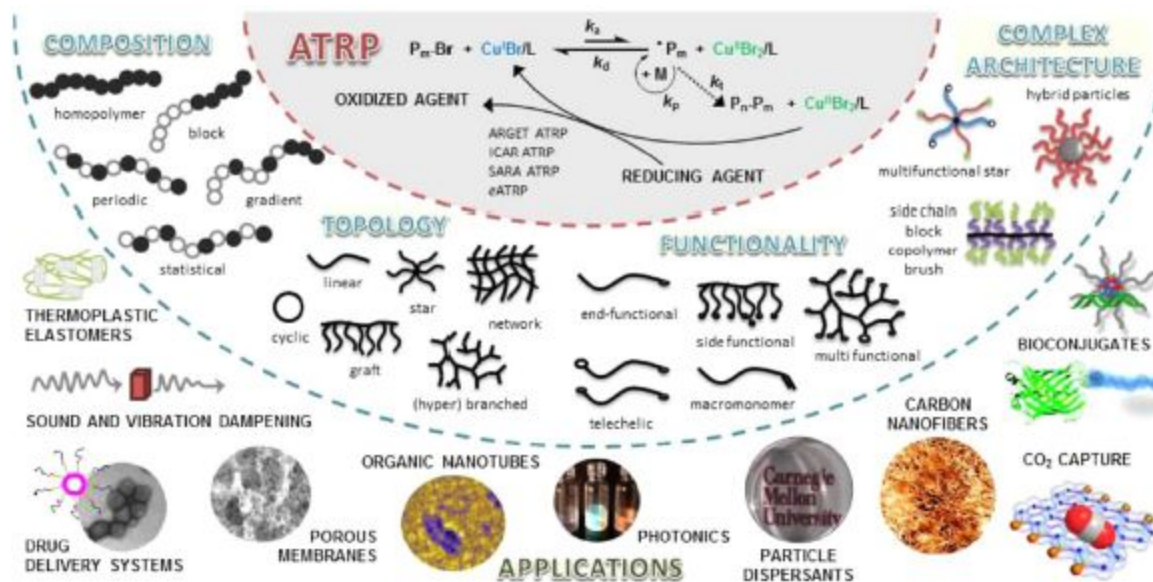
## Macromolecular Engineering by Atom Transfer Radical Polymerization

Krzysztof Matyjaszewski<sup>\*,†</sup> and Nicolay V. Tsarevsky<sup>‡</sup>

<sup>†</sup>Department of Chemistry, Carnegie Mellon University, 4400 Fifth Avenue, Pittsburgh, Pennsylvania 15213, United States

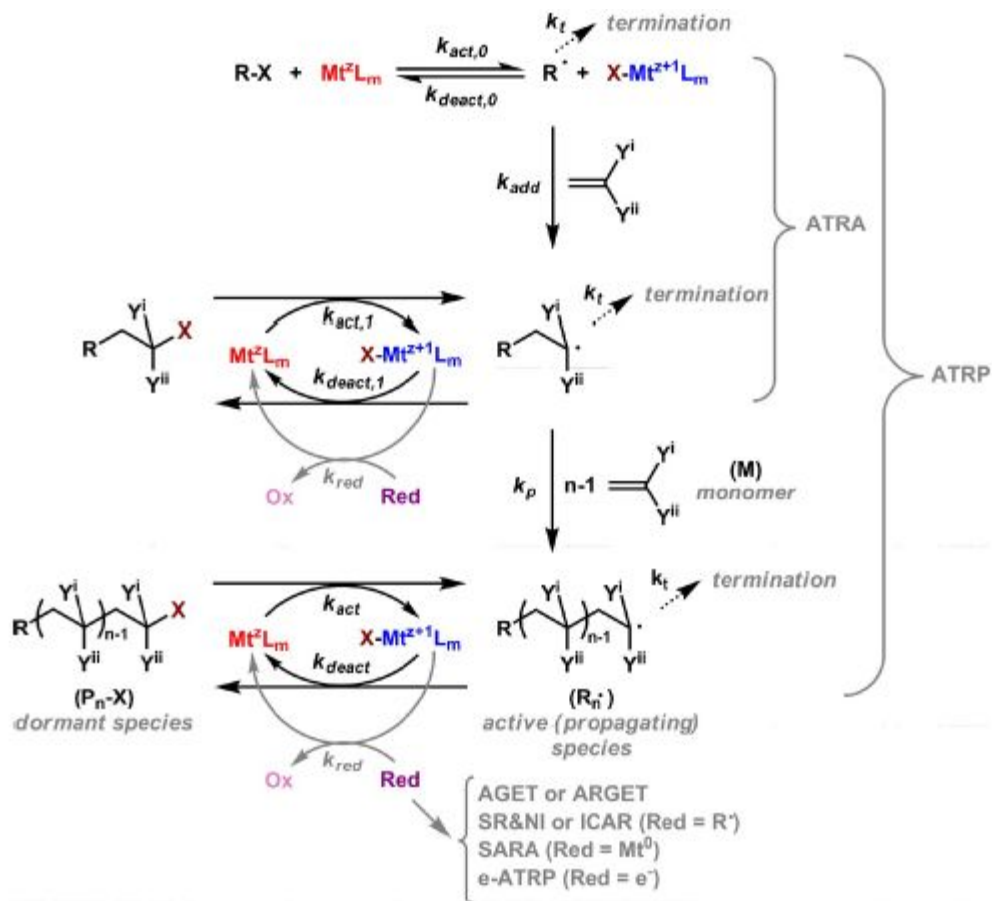
<sup>‡</sup>Department of Chemistry and Center for Drug Discovery, Design and Delivery in Dedman College, 3215 Daniel Avenue, Southern Methodist University, Dallas, Texas 75275, United States

Возможности метода радикальной полимеризации с переносом атома (ATRP) с использованием Си-содержащих агентов в аспекте создания новых структурных типов макромолекул и их применений



Scheme 1. Overview of New ATRP Techniques with ppm Amounts of Cu Catalysts, Engineering Macromolecular Architecture, and Applications of Resulting Materials<sup>42</sup>

# Механизм обычного процесса ATRP и процесса ATRP в присутствии восстановителя



Scheme 2. Mechanism of Transition Metal Complex-Mediated ATRA and ATRP and Low-Catalyst-Concentration ATRA and ATRP Techniques in the Presence of Excess of Reducing Agents

Влияние экранирующих (a) и стабилизирующих (b) заместителей и природы атома галогена (c) на значение константы равновесия  $K_{ATRP}$

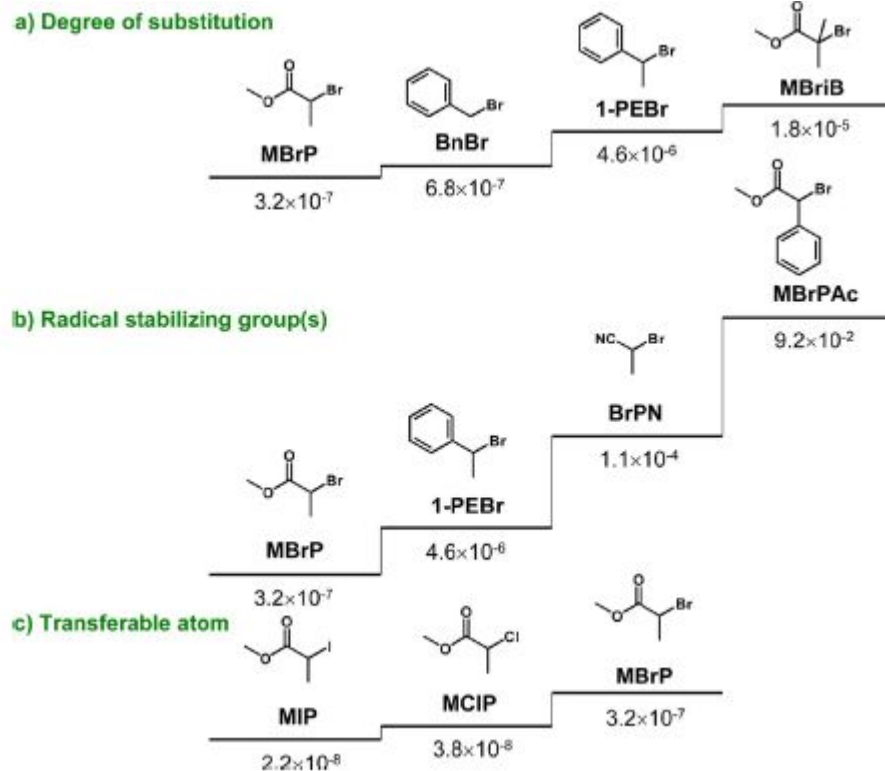


**Figure 1.** Effects of the degree of substitution (a), type of radical stabilizing groups (b), and nature of the transferable atom (c) on the values of  $K_{ATRP}$  for the reaction between various alkyl halides and the  $Cu^I$  complex of tris(2-pyridylmethyl)amine (TPMA) in acetonitrile at 22 °C. Data from ref 26a.

Молекулярно-массовое распределение и функциональность  
макромолекул,  
полученных методом ATRP

$$\frac{M_w}{M_n} = 1 + \frac{1}{DP_n} + \left( \frac{[R-X]_0 k_p}{k_{deact}[X-Cu^{II}L_m]} \right) \left( \frac{2}{conv.} - 1 \right) \quad (1)$$

$$\begin{aligned} DCF &\equiv \frac{[T]}{[R-X]_0} \\ &= \frac{2DP_{n,targ} k_t [\ln(1 - conv.)]^2}{[M]_0 k_p^2 t} \\ &= \frac{2k_t [\ln(1 - conv.)]^2}{[R-X]_0 k_p^2 t} \end{aligned}$$

## Влияние структуры лиганда в комплексе меди на константу равновесия $K_{\text{ATRP}}$

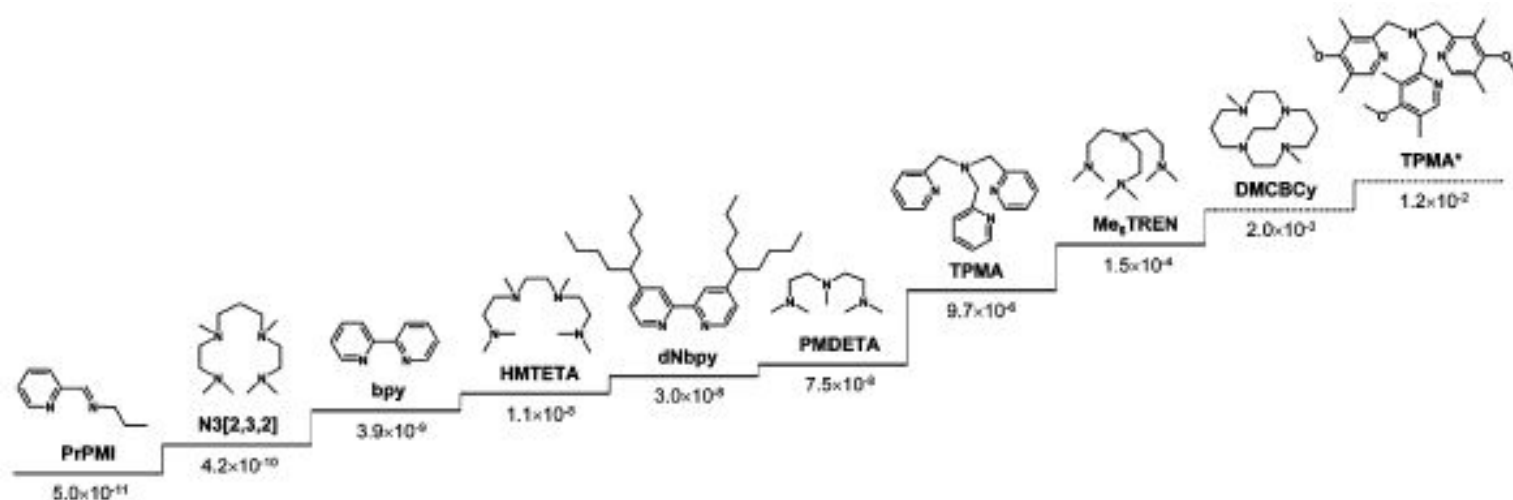


**Figure 2.** Effect of the ligand on the value of  $K_{\text{ATRP}}$  for the reaction between ethyl 2-bromoisobutyrate and Cu<sup>I</sup> complexes in acetonitrile at 22 °C. The value for the DMCBCy<sup>17</sup> complex was estimated on the basis of the differences in reactivities of the Cu<sup>I</sup> complexes of Me<sub>6</sub>TREN and DMCBCy toward methyl chloroacetate and those of the Cu<sup>I</sup> complex of Me<sub>6</sub>TREN toward methyl chloroacetate and ethyl 2-bromo isobutyrate. The value for the TPMA\* complex is estimated on the basis of the differences in reactivities of the Cu<sup>I</sup> complexes of TPMA and TPMA\* toward MBrP and those of the Cu<sup>I</sup> complex of TPMA toward MBrP and ethyl 2-bromoisobutyrate. Data from ref 22b and 26a.

## Влияние природы растворителя на константу равновесия

$K_{\text{ATRP}}$

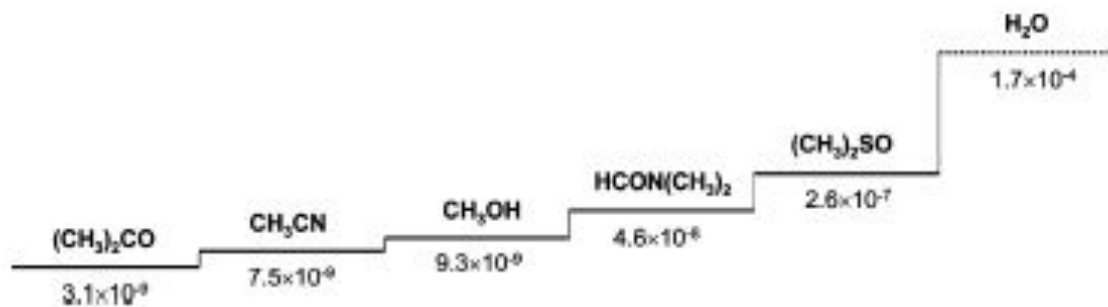


**Figure 3.** Effect of solvent on the value of  $K_{\text{ATRP}}$  for the reaction between 2-bromoisobutyrate with the  $\text{Cu}^{\text{I}}$  complex of HMTETA at 25 °C. The value for water was estimated from the equilibrium constant for the  $\text{Cu}^{\text{I}}$  complex of TPMA and the ratio of the reactivities of the HMTETA and TPMA complexes toward ethyl 2-bromoisobutyrate in acetonitrile. Data from ref 20.

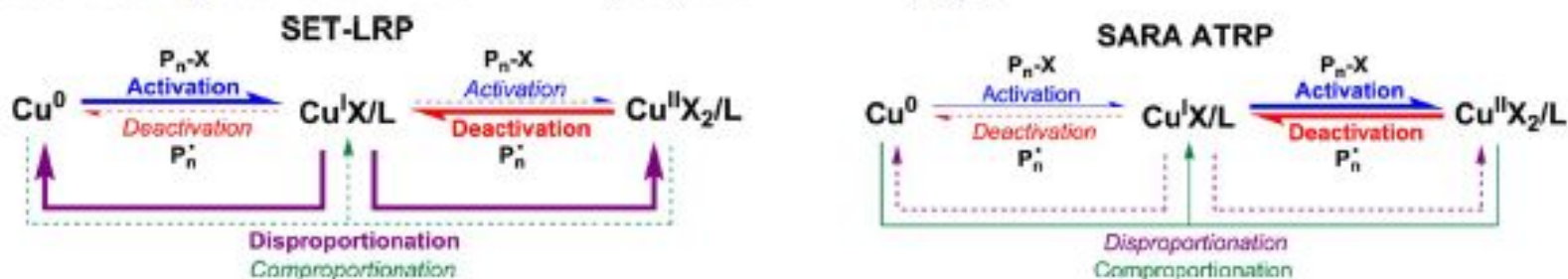


## Скорость полимеризации

$$R_p = k_p[M][R^*] = k_p K_{\text{ATRP}} \frac{[M][P-X][Mt^2 L_m]}{[X-Mt^{2+1} L_m]}$$

## Схема процессов «SET ATRP» и «SARA ATRP»

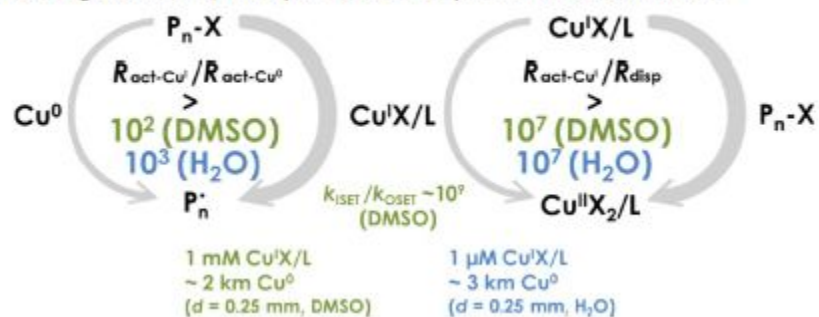
Scheme 3. Proposed Mechanisms of SET ATRP (Left) and SARA ATRP (Right)<sup>44</sup>



<sup>44</sup>The line thickness corresponds to the values of rates of the corresponding reactions; dotted lines indicate the slowest reactions that can be kinetically neglected. For simplicity,  $P_n^*$  formed in activation,  $P_n^*X$  formed in deactivation and stoichiometry for disproportionation/comproportionation are neglected. In the originally proposed SET-LRP, no activation by  $Cu^I$  or comproportionation took place.<sup>45</sup> In SARA ATRP, absolute values of the rates determined at ca. 70% conversion in MA polymerization in DMSO ( $[MA]_0:[MBrP]_0:[Me_6TREN]_0 = 200:1:0.1$ , MA/DMSO = 2/1 (v/v),  $V = 4.5$  mL,  $S = 1.27$  cm<sup>2</sup> ( $l = 4$  cm,  $d = 1$  mm),  $T = 25$  °C) are ca.  $3 \times 10^{-3}$  M/s (propagation, activation by  $Cu^I$  and deactivation by  $Cu^0$ ),  $10^{-6}$  M/s (termination and supplemental activation by  $Cu^0$ ),  $10^{-7}$  M/s (comproportionation),  $10^{-9}$  M/s (deactivation by  $Cu^I$ ), and  $10^{-10}$  M/s (disproportionation).<sup>48</sup>

## Сравнение скоростей активации галоидалкилов в присутствии $\text{Cu}^0$ $\text{Cu}^1$ при полимеризации акрилатов в ДМСО и воде

Scheme 4. Comparison of Activation Rates of Alkyl Halides (Left, by  $\text{Cu}^0$  and Right, by  $\text{Cu}^1$ ) and Role of  $\text{Cu}^1$  (Left, Disproportionation and Right, Activation) in Polymerization of Acrylates in DMSO and in Water<sup>a</sup>



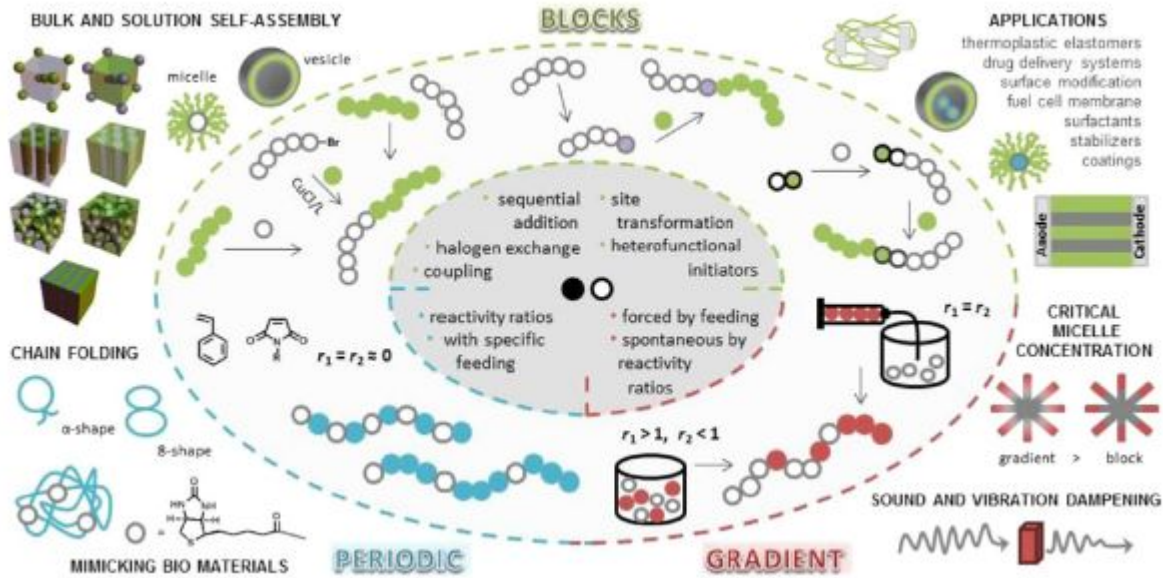
<sup>a</sup>Bottom part illustrates unrealistic lengths of  $\text{Cu}^0$  wire ( $d = 0.25$  mm) needed to match activity of  $[\text{Cu}^1/\text{Me}_6\text{TREN}] = 1$  mM in DMSO and  $[\text{Cu}^1/\text{Me}_6\text{TREN}] = 1$   $\mu\text{M}$  in water.

## Средства настройки процесса ATRP

- Структура мономера, выбор атома галогена;
- Инициатор (тип, концентрация)
- Агент переноса атома (тип агента, концентрация);
- Комплексообразователь (хим. строение, концентрация);
- Растворитель (тип, концентрация);
- Восстановитель;
- Температура.

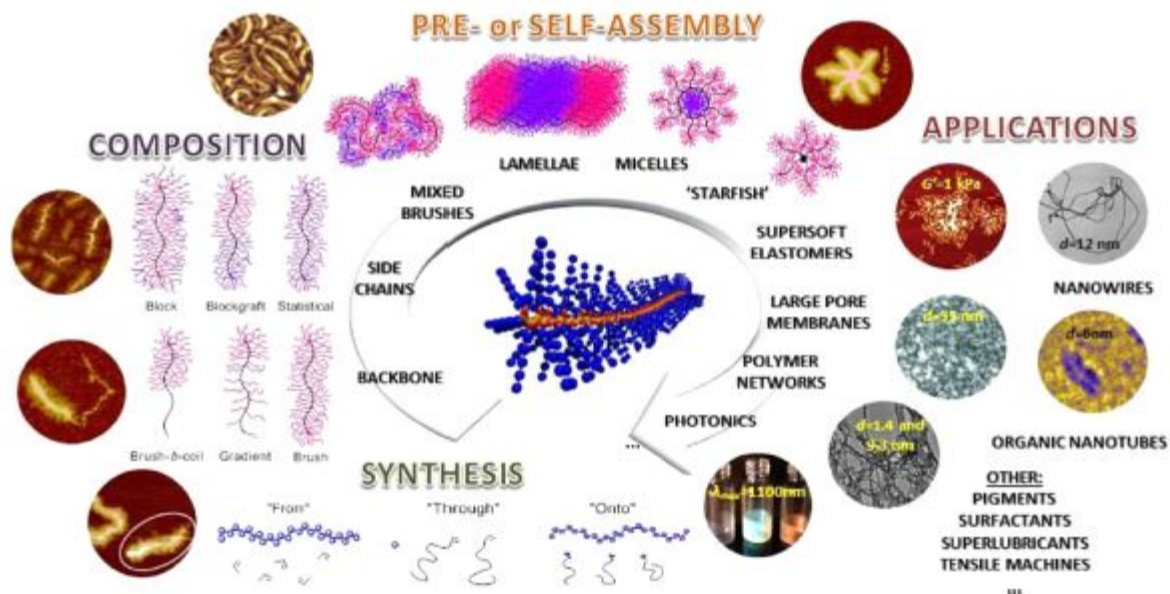
# Способы получения блок-градиентных и периодических полимеров и их применение

Scheme 5. Synthetic Routes for the Preparation of Block, Gradient, and Periodic Copolymers and Their Applications



# Молекулярные «ершики»: синтез и применение

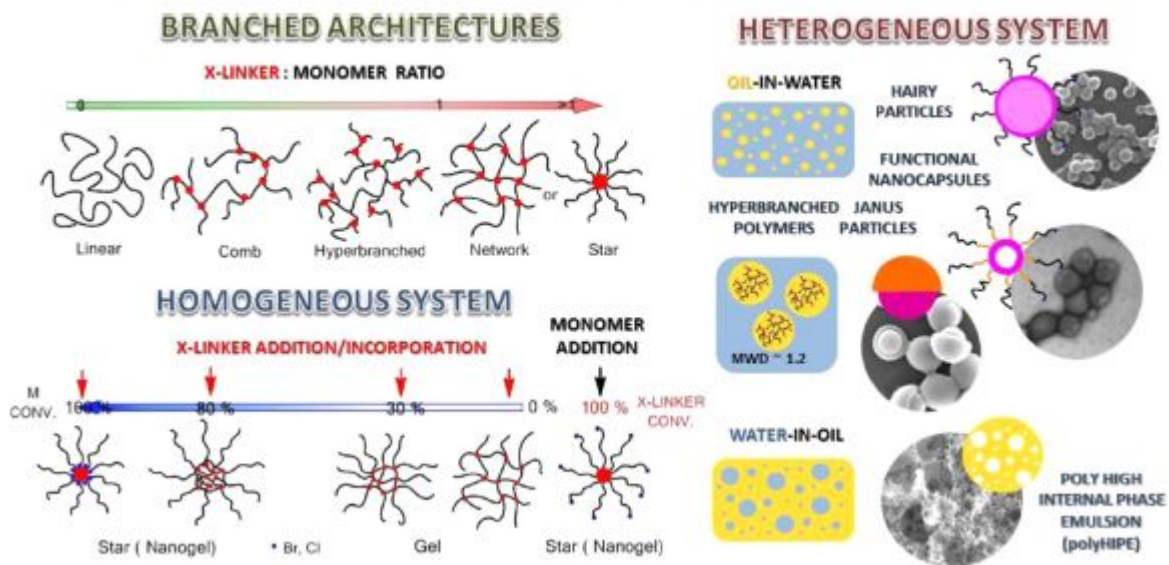
Scheme 6. Molecular Bottlebrushes with Various Composition and Architecture, Their Properties, and Potential Applications<sup>a</sup>



<sup>a</sup>Adapted with permission from refs 90, e, and 92.

# Синтез полимеров разветвленной структуры сополимеризацией мономера и сшивающего агента

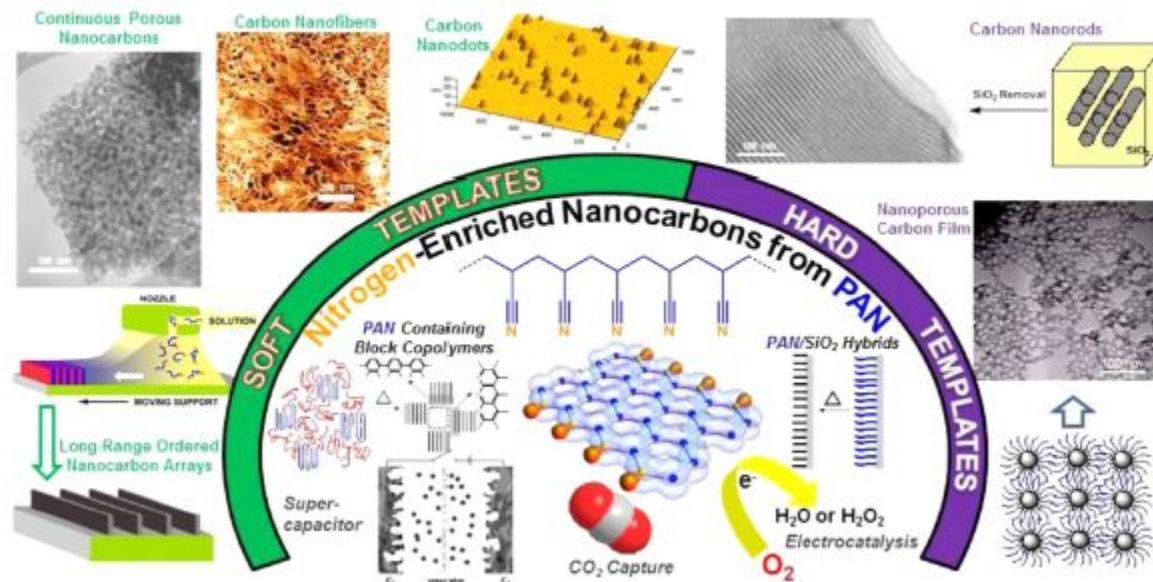
Scheme 7. Polymers with Branched Architectures via Copolymerization of Monomer and Cross-linker<sup>a</sup>



<sup>a</sup>Structures depend on the cross-linker:monomer ratio and the moment of cross-linker incorporation. Adapted with permission from refs 9b and 102.

# Получение наноструктурированных углеродных материалов с использованием метода ATRP

Scheme 8. Preparation of Multifunctional N-Enriched Nanostructured Carbon Materials from Polyacrylonitrile-Based Precursors Engineered via ATRP<sup>42</sup>

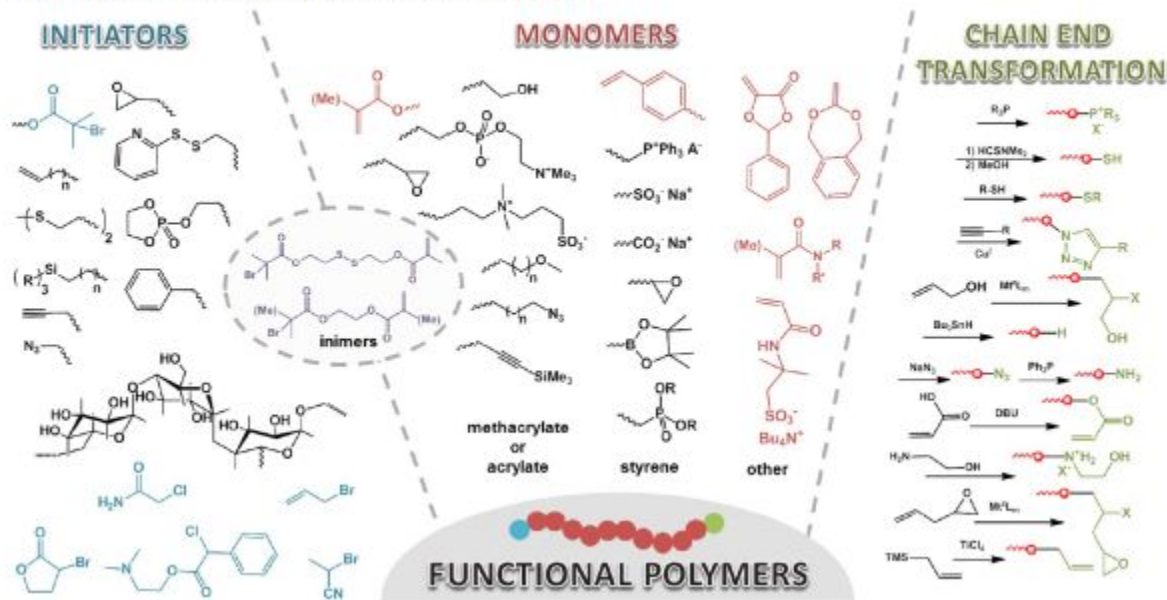


<sup>42</sup>In the center is shown polyacrylonitrile (PAN), a semi-crystalline polymer, as a precursor for partially graphitic carbon materials. The carbonization involves stabilization under air at >200 °C and fusing ladder structures under Ar or N<sub>2</sub> above 500 °C. Above the arc, to the left is shown soft templating based on the self-assembly of PAN block copolymers: carbon nanodots from pre-assembled poly(acrylic acid)-*b*-PAN micelles, with PAA outer-shells; carbon nanofibers from phase-separated PnBA-*b*-PAN copolymer with a cylindrical morphology, with PBA as a sacrificial block; PBA-*b*-PAN with a bicontinuous morphology for continuous porous nanocarbons; and zone-casting to form long-range ordered lamellar carbon arrays. To the right is shown hard templating with etchable SiO<sub>2</sub>: PAN grafted from the concave surface of mesoporous silica, yielding carbon nanorods ( $d = 10$  nm); and nanoporous carbon films synthesized from PAN grafted from silica nanoparticles, with mesopores ( $d = 15$  nm) after etching silica. Below the arc, it is shown that the partially graphitic nanocarbons contain pyridinic N-atoms at the graphene edges with potential applications: electrode materials for supercapacitors mediating reversible proton-coupled ET, sorbents for selective CO<sub>2</sub> capture, and electrocatalysts for oxygen reduction reaction via a four-electron-transfer process with the same overpotential as a Pt catalyst. Adapted with permission from refs 9d and 105.



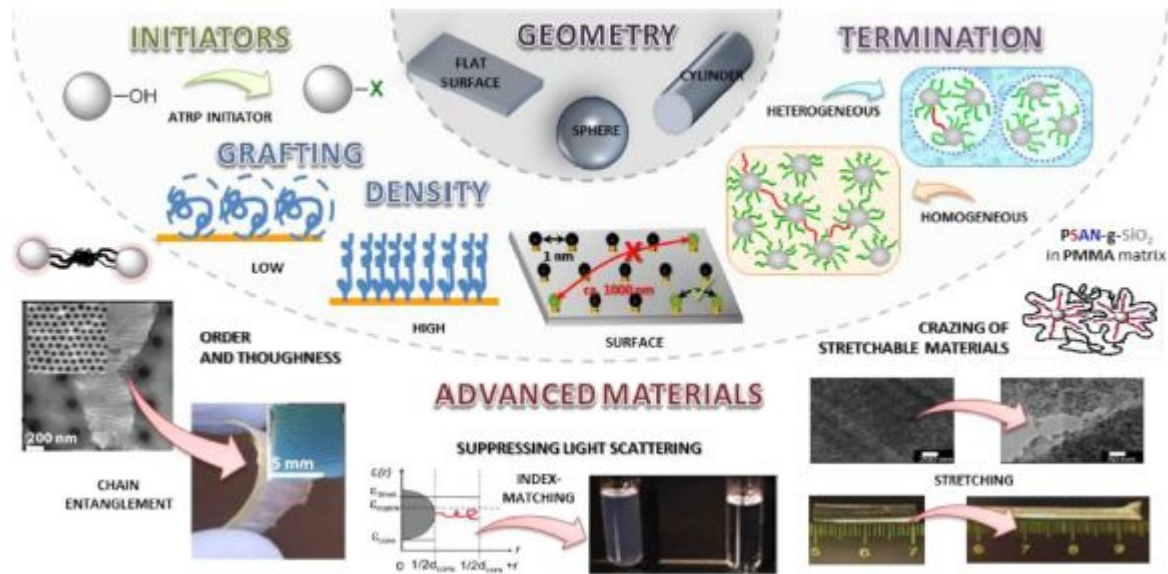
# Получение полимеров с концевыми функциональными группами методом ATRP

Scheme 9. Examples of Molecules Used To Form Functional Polymers by ATRP, from Functional Initiators (Blue), Monomers (Red), and Inimers, and by Chain End Transformation (Green)



# Получение хорошо охарактеризованных полимерно-неорганических гибридов методом SI ATRP

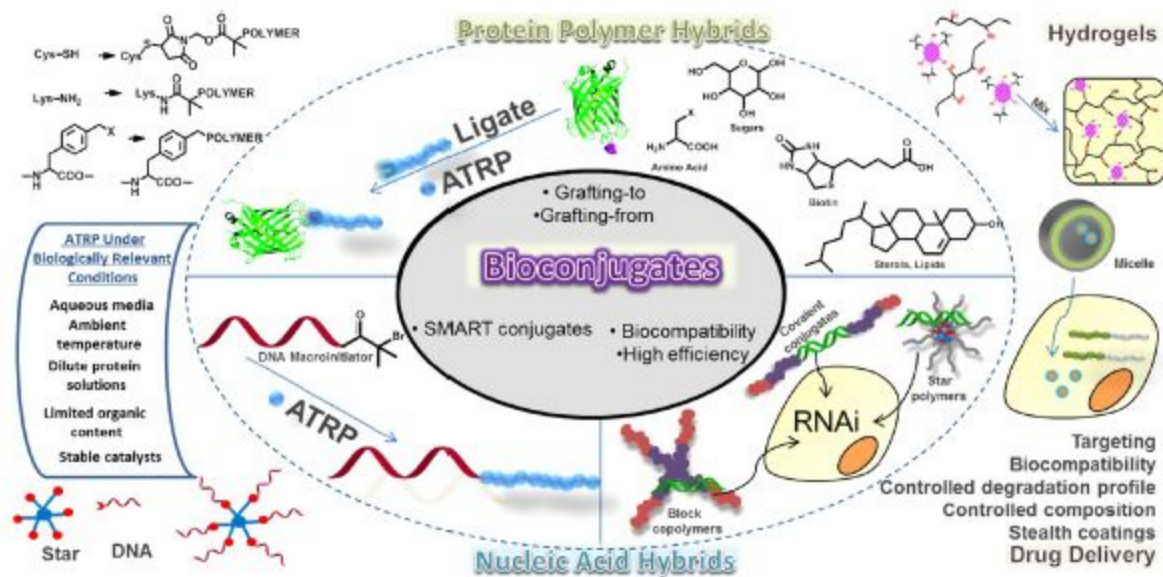
Scheme 10. Synthesis of Well-Defined Polymer/Inorganic Hybrids via SI ATRP and Some Examples of Hybrid Materials<sup>44</sup>



<sup>44</sup>Shown are surface modification of inorganic supports with various geometries and composition with tetherable ATRP initiators; control of grafting density by tetherable initiators with either ATRP active or inactive sites; principle of termination on flat surfaces via "migration effect" and suppression of macroscopic gelation in miniemulsion; self-assembly of tough hybrids (via chain entanglement) into ordered photonic materials with strong iridescence; null scattering by matching the overall refractive index of hybrids with that of a solvent or polymeric matrix; and stretchable and optically clear materials with 70 wt% silica based on blends of hybrids with short poly(styrene-*co*-acrylonitrile) (PSAN)-grafted brushes ( $DP = 20$ ), dispersed in PMMA matrix. Adapted with permission from refs 9a, 125, and 131.

# Получение биоконъюгатов методом ATRP

Scheme 11. Bioconjugates Prepared by ATRP



## Перспективы метода ATRP

